ELSEVIER

Journal of Power Sources 113 (2003) 355–362

JOURNAL OF POWER SOURCES

www.elsevier.com/locate/jpowsour

Influence of charge mode on the capacity and cycle life of lead–acid battery negative plates

G. Petkova, D. Pavlov*

Central Laboratory of Electrochemical Power Sources, Bulgarian Academy of Sciences, 1113 Sofia, Bulgaria

Abstract

The effect of fast and three-step charge mode on the capacity and cycle life of lead–acid battery negative plates was investigated using a model mini electrode (ME). It has been found that the charge algorithm exerts a strong effect on the charge acceptance of the negative electrode. In the two-step charging mode I_1, φ_2 with increase of the current at the first step of charge, the capacity of the negative electrode decreases and the cycle life shortens. This phenomenon is reversible as it is probably due to the incomplete reduction of $PbSO_4$ to Pb. The phenomenon is explained based on the mechanism of the process of reduction of $PbSO_4$. At high initial charge currents, the concentration of H_2SO_4 in the pores of NAM increases, which decreases the solubility of $PbSO_4$ crystals and limits the charge acceptance of the negative plate. The higher initial charge current influences markedly the formation of smaller Pb crystals that build up the energetic structure of the negative active material. It is essential that a third step with a small constant current, I_3 is added to the charge algorithm. The third step of charge in the I_1, φ_2, I_3 charge mode decreases the Ohmic resistance and ensures complete charge of the lead electrode.

Keywords: Lead–acid batteries; Charging regime; Cycle life; Lead negative electrode

1. Introduction

Fast charging of batteries has become a widely applied technique for improvement of the cycle-life performance of VRLA batteries with PbSnCa grids. The beneficial effect of fast charging on the positive active mass (PAM) structure and on the cycle life of the positive plates has been the subject of many papers. However, the effect of high rate of charge on the structure of the negative active mass (NAM) and on the electrical characteristics of the negative plate has not been clearly elucidated yet.

Recently, attention has been drawn to the decline in negative plate capacity of VRLA batteries on cycling [1,2]. It has been found that this capacity decay is a result of reduced charging efficiency and formation of so-called "hard sulfate", which is difficult to reduce to Pb. A final constant current step without voltage limit has been recommended as an equalizing step for VRLA batteries to ensure sufficient recharge of the negative electrode [3–6]. Also, a charge algorithm with a current-interrupt finishing step has been proposed as a tool for extending the life on deep cycling [7].

The aims of the present work are to discover the phenomena that limit the charge acceptance during fast charge of the negative plate, to study the effect of the three-step charge mode on the capacity and cycle life, and to optimize the charge mode of the lead–acid battery.

2. Experimental

2.1. Electrodes

The investigation was performed using a model mini electrode (ME) [8] presented diagrammatically in Fig. 1. The base of the Pb–0.1% Ca spine inserted in a PTFE holder was covered with a conventional negative paste. The paste containing 0.2% organic expander, 0.2% carbon black, and 0.8% $BaSO_4$ had a density of 4.2 g cm^{-3}. Preparation of the ME followed standard curing and formation procedures. A sheet of AGM separator was placed over the negative active mass and then pressed with a PTFE cap. This construction confines the expansion of the NAM during cycling.

2.2. Cell

The experiments were carried out in a classical three-electrode cell with a ME as working electrode, a Hg/Hg_2SO_4 reference electrode and a small lead plate as counter electrode. All potential measurements were performed

* Corresponding author. Tel.: +359-2-718651; fax: +359-2-731552.
E-mail address: dpavlov@mbox.cit.bg (D. Pavlov).

0378-7753/02/$ – see front matter
PII: S0378-7753(02)00548-7

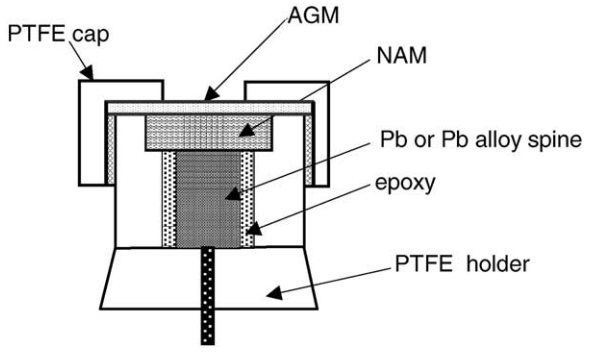

Fig. 1. Model electrode (ME) construction.

versus Hg/Hg_2SO_4 reference electrode. The electrodes were cycled in an excess of 1.28 s.g. H_2SO_4 at ambient temperature.

The tests were performed using an Arbin BT2043 potentiostat/galvanostat.

2.3. Charge modes

The model electrodes were charged using two different charge algorithms:

(i) I_1, φ_2: two-step mode with a constant current I_1 until the potential φ_2 is reached, then the charge continues at a constant potential φ_2 to charge factor $C_F = 1.15$.
(ii) I_1, φ_2, I_3: three-step mode with a constant current I_1 to potential φ_2 followed by a constant potential (φ_2) step until the current falls down to I_3 and a third step with a constant current I_3 to charge factor $C_F = 1.15$.

The ME electrode was discharged at $C/3$ rate down to −0.75 V, which corresponds to 100% DOD. Initially, the MEs were subjected to three capacity cycles at a 20-h rate of discharge. The electrodes were cycled until the 60 mAh g capacity was reached.

3. Results and discussion

3.1. I_1, φ_2: two-step charge mode

Fig. 2 shows the potential and current transients during discharge and charge of the ME when the two-step algorithm was applied.

Two different initial currents, $I_1 = 0.5$ and 1.0 C A, were applied with a potential limited to $\varphi_2 = -1.1$ V. It can be seen from the figure that the high initial charge current ensures faster charge return to 100% state of charge, than the lower one. The current during the second step falls to very low values and this step takes a fairly long time period of recharge. It is important to notice that at the end of the first step, the state of charge is around 75% on fast charge, while on slow charge it is around 90%.

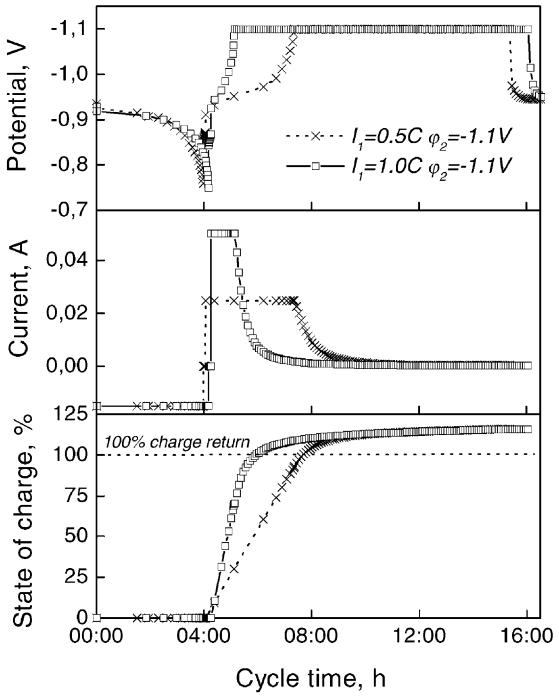

Fig. 2. Charge mode I_1, φ_2.

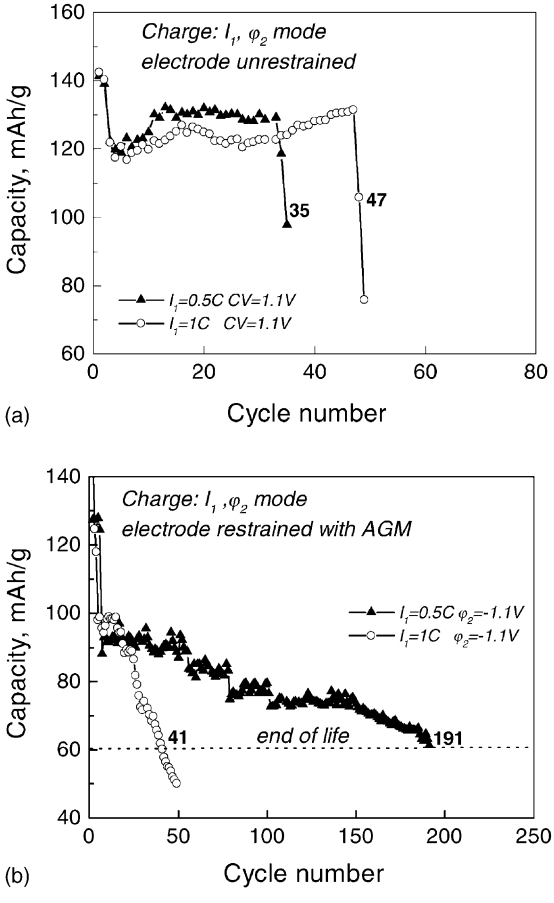

Fig. 3. Influence of the initial charging current I_1 on the cycle life of the negative electrode. (a) Free expanded NAM; (b) NAM confined by AGM sheet.

3.2. Influence of charge mode on the cycle life

Fig. 3 presents the capacity of the model electrode as a function of cycle number at two different I_1 currents. When the NAM is not confined (Fig. 3a) the capacity delivered by the electrode is relatively high, around 130 mAh g, but in this case the cycle life of the electrodes is very short. The fast charge of the electrode yields a bit longer cycle life. The reason for the steep decline in capacity and hence for the end of cycle life proved to be swelling of the active material and loss of contact between the metal substrate and the negative active material.

The picture changes for the model electrode confined by an AGM sheet (Fig. 3b). In this case, the capacity delivered by the electrode is lower as compared to the unconfined electrode. When the first charge step is conducted with $I_1 = 1.0$ C A, the cycle life of the model electrode is short. On charge with $I_1 = 0.5$ C A, the ME reaches 60 mAh g capacity for about 191 cycles.

Evidently, both the capacity and cycle life depend strongly on the design of the cell and the charge regime. It can be assumed that there is an optimum NAM pore volume, which ensures maximum electrode capacity and longest cycle life at a certain charge regime.

Fig. 3b shows that the value of the initial charge current I_1 markedly influences the capacity and cycle life of the plates. The question arises whether the above effect is reversible. Fig. 4 shows the capacity of the ME as a function of cycle number on charge with $I_1 = 0.5$ C A. Periodically, the electrode was charged with $I_1 = 1$ or 1.5 C A. It can be seen, that when the charge current $I_1 = 0.5$ C A is changed to $I_1 = 1$ C A the capacity decreases. At initial charge current $I_1 = 1.5$ C A, the capacity decrease is greater than when the electrode is charged with $I_1 = 1$ C A. On switching to the $I_1 = 0.5$ C A charge mode, the capacity restores its initial value after some cycles. This indicates that the structure of NAM depends reversibly on the value of the charge current at the first step, when a great part of $PbSO_4$ is reduced to Pb.

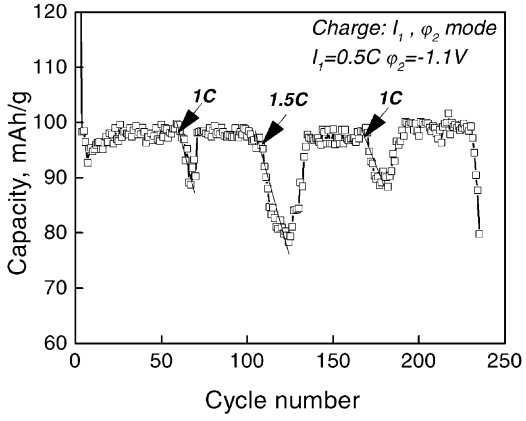

Fig. 4. Influence of the initial charging current on the capacity of the negative electrode.

3.3. Mechanism of the processes of residual sulphation of the negative plate that limit its charge acceptance

The XRD patterns of the NAM in charged state after two-step charge with three different initial charge currents ($I_1 = 0.5$, 1 or 1.5 C A) are presented in Fig. 5. The results evidence the presence of some amount of $PbSO_4$ after charge with $I_1 = 1$ and 1.5 C A. Thus an increase of the I_1 current leads to incomplete recharge of the negative active material at this charge mode. Residual $PbSO_4$ is found in the inner layers of the plate.

The occurrence of this residual sulphation of the inner layers of the negative plate can be explained on the basis of the mechanism of $PbSO_4$ reduction to Pb and the dependence of $PbSO_4$ solubility on the concentration of H_2SO_4 in the pores of the NAM. The mechanism of $PbSO_4$ reduction to Pb comprises the following elementary processes:

(a) Dissolution of $PbSO_4$ crystals to Pb^{2+} and SO_4^{2-} ions.
(b) Diffusion of Pb^{2+} ions to the active centers where the electrochemical reaction of Pb^{2+} reduction to Pb proceeds.
(c) Surface diffusion of Pb atoms to the sites of Pb nucleation and crystal growth.
(d) Diffusion and migration of SO_4^{2-} ions out of the pores of NAM. This step is very slow as the SO_4^{2-} ions have but a very low mobility. Electroneutralization of the SO_4^{2-} ions proceed through diffusion and migration of H^+ ions from the bulk solution into the pores of the NAM. The H^+ ions have 10 times higher mobility than SO_4^{2-} ions. The electrochemical reaction continues

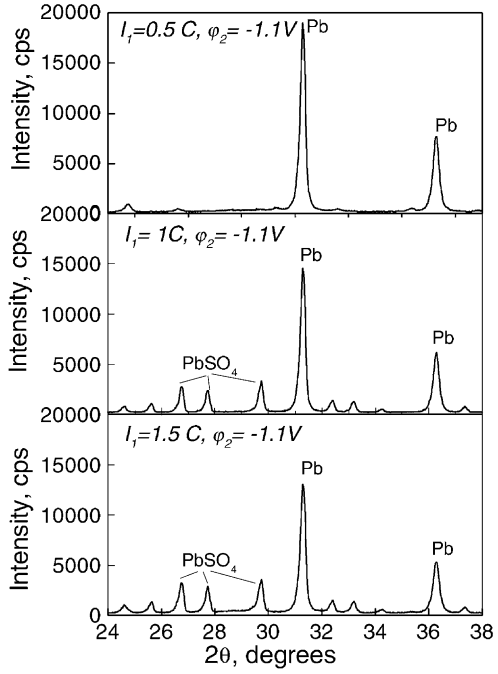

Fig. 5. XRD patterns for samples charged with different initial charge currents I_1 in the I_1, φ_2 charge mode.

only at the sites of the NAM where the SO_4^{2-} ions are electrically neutralized. If the negative charges of the SO_4^{2-} ions generated by the electrochemical reaction are not neutralized, the pore volume will be charged negatively and the electrochemical reaction will stop at this particular site.

(e) The H_2SO_4 concentration in the pores increases and a concentration gradient is formed between H_2SO_4 in the pores and the bulk of the electrolyte. Under its action, H_2SO_4 diffuses towards the bulk solution. This is a slow process.

The solubility of $PbSO_4$ crystals depends strongly on the concentration of sulfuric acid. Vinal and Craig [9], and Danel and Plichon [10] have established that on increase of $C_{H_2SO_4}$ from 1.12 to 1.30 s.g., the solubility of $PbSO_4$ decreases about five times (Fig. 6).

When the charge current is high the concentration of H_2SO_4 in the pores of the NAM increases rapidly and the solubility of $PbSO_4$ declines. The Pb^{2+} concentration in the volume of the pores decreases and the rate of the electrochemical reaction is slowed down. Thus the charge acceptance of the negative plate is limited by the rate of dissolution of $PbSO_4$ crystals. The charge efficiency will depend on the rate of H_2SO_4 diffusion out of the NAM pores. The diffusion of H_2SO_4 towards the bulk solution depends on the pore structure of the negative active material. Hence, the compression of the negative plate has a negative effect on its charge acceptance. The results presented in Fig. 3 support the above mechanism. Besides, the residual sulphation of the negative plate will depend on the charging mode and the volume and concentration of H_2SO_4 in the cell.

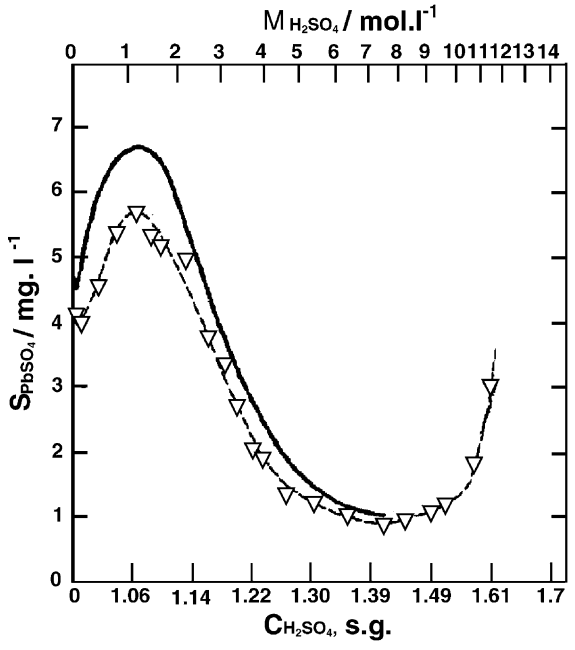

Fig. 6. Dependence of $PbSO_4$ solubility on H_2SO_4 concentration according to (—) Vinal and Craig [9], and (▽) Danel and Plichon [10].

On charge with low initial current, when the local H_2SO_4 concentration in the pores of NAM increases due to slow diffusion of H_2SO_4, the electrochemical reaction may start to proceed at other sites where $C_{H_2SO_4}$ is low. This self-regulation of the processes in the NAM volume will maintain a high charge acceptance. Moreover, the time of H_2SO_4 diffusion out of the plate is sufficient to keep the H_2SO_4 concentration in the plate interior not much higher than that in the bulk of the electrolyte.

The existence of residual sulphation has been observed on cycling of positive plates as well [11].

3.4. Effect of charge current on the structure of the negative active mass

The negative active mass comprises a skeleton, which conducts the current, and small lead crystals on the surface of the skeleton, which take part in the charge/discharge processes and form the so-called energetic structure [12]. The micrographs in Fig. 7a and b present the energetic structure of NAM at the end of cycle life on cycling with a two-step charging mode with $I_1 = 0.5$ or 1 C A, respectively. It can be seen that smaller crystals are formed on charge with high initial current than the ones formed on cycling with low charge current. This suggests, that the initial charge current affects the nucleation and growth processes of metallic lead. In the case of fast charge, though the electrode was fully charged, some $PbSO_4$ crystals can be seen in the pores of NAM. This is in accordance with the XRD data (Fig. 5).

The NAM skeleton structures presented in Fig. 7c and d were obtained employing the procedure developed earlier, i.e. the $PbSO_4$ crystals, formed on plate discharge, were dissolved in a hot solution of CH_3COONH_4 [12]. Thus the skeleton structure of NAM is demonstrated. On comparing the skeleton structures of the two electrodes, it can be seen that larger pores are formed on cycling with low I_1. This type of structure allows the H_2SO_4 formed in the pores during charge to leave the plate faster, and hence ensures higher charge acceptance.

3.5. I_1, φ_2, I_3: three-step charge mode

The effect of the constant current finishing step on the cycle life of the negative electrode was investigated. A step with a constant current $I_3 = 0.05$ C A was included in the fast charge algorithm for the negative electrode.

Fig. 8 shows the potential and current transients during charge of the ME employing a three-step charge algorithm. The negative electrode is almost 100% charged when the constant current finishing step starts. During this step the potential of the negative electrode rises above −1.20 V, which is an evidence that the reaction of hydrogen evolution proceeds.

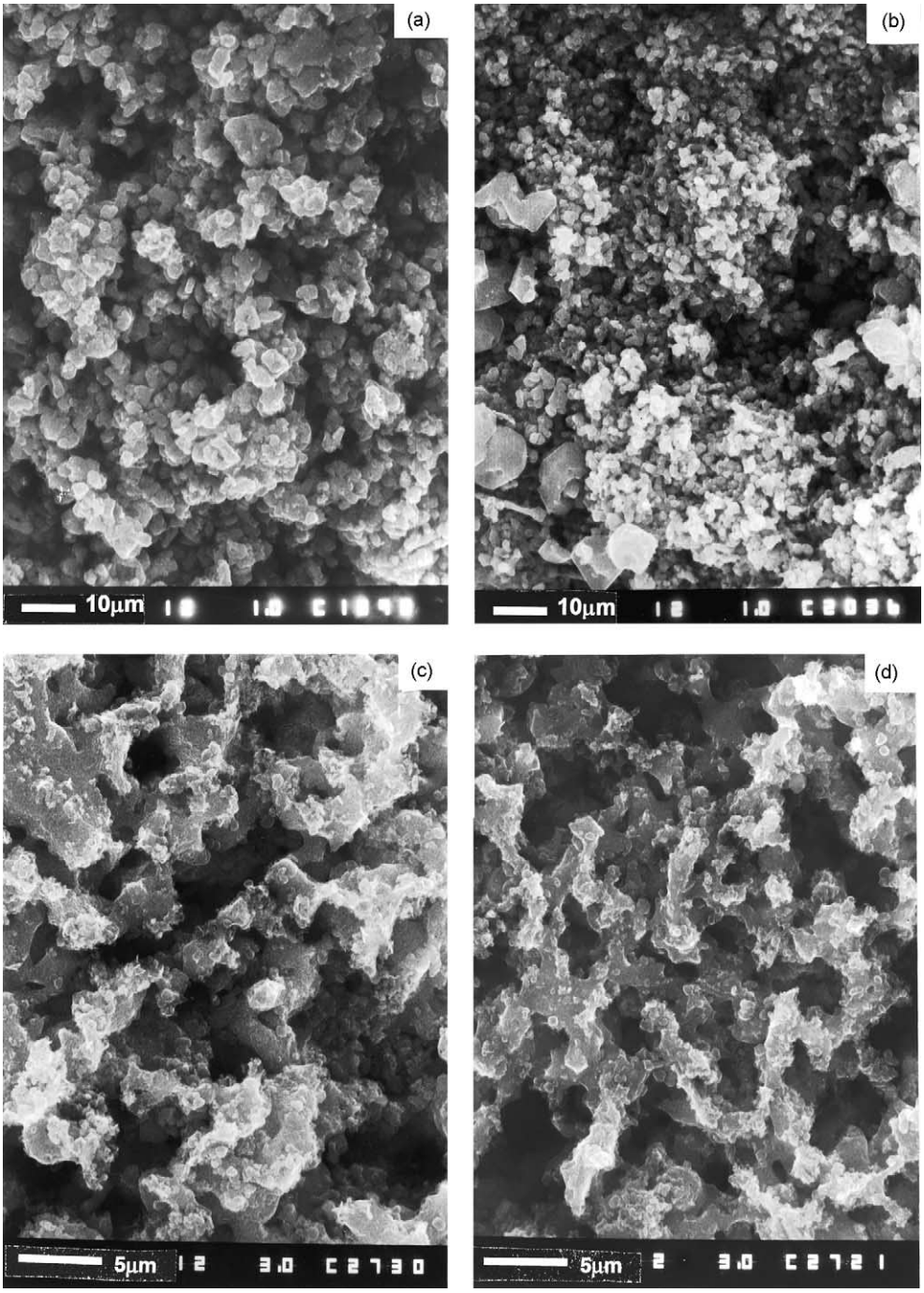

Fig. 7. SEM micrographs of the NAM after the end of cycle life: (a, c) charge $I_1 = 0.5$ C A, $\varphi_2 = -1.1$ V; (b, d) charge $I_1 = 1$ C A, $\varphi_2 = -1.1$ V; (a, b) energetic structure; (c, d) skeleton structure.

3.6. Effect of the three-step charge mode on the cycle life of the negative plate

We tried to trim down the negative effect of the charge with high I_1 current on the capacity of lead–acid battery negative plates through optimization of the second and third charge steps. Fig. 9 presents the dependencies of the ME capacity on the number of cycles when a three-step charge mode was applied with two values of the current I_3. It is evident that charging with higher final current leads to a decline in cycle-life performance. Values of $I_3 \approx 0.05$ C A are appropriate for improving the cycle life of the negative electrode.

A comparison between the capacity/number of cycles curves in Fig. 9 and those presented in Fig. 3b indicates that the role of the third step is very important on charge with

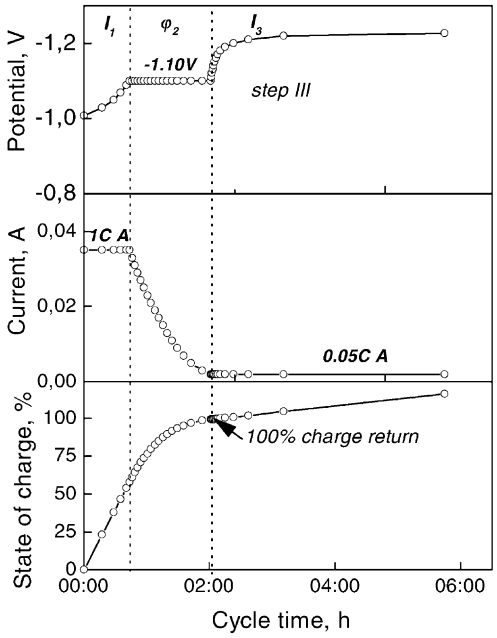

Fig. 8. Potential/time transients on I_1, φ_2, I_3 charge.

high initial current $I_1 = 1$ C A. When the two-step charge mode is applied the capacity decreases and the cycle life of the negative electrode is shortened (Fig. 3b). The cycle life can be prolonged by including a third step in the charge algorithm, $I_3 = 0.05$ C A. During this step the $PbSO_4$ in the negative plate is completely reduced to Pb.

The resistance of the model electrode was determined during the final step of charge using Arbin software for internal resistance measurements employing a pulse technique. It can be seen from Fig. 10 that during the third constant current step, the resistance of the negative electrode decreases. This resistance decrease depends on the potential at the second charge step. With increase of the potential, φ_2, the resistance of the electrode during the third charge step decreases.

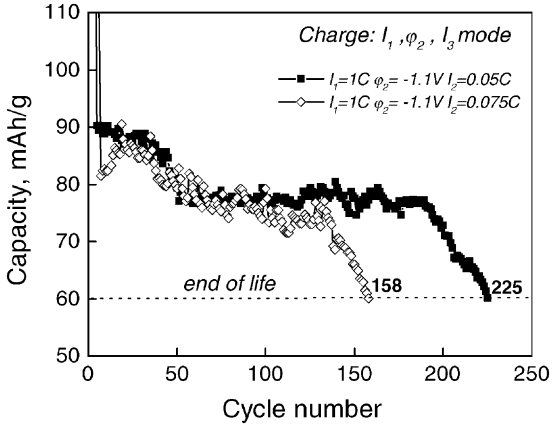

Fig. 9. Influence of the I_3 current on the cycle life of the negative electrode.

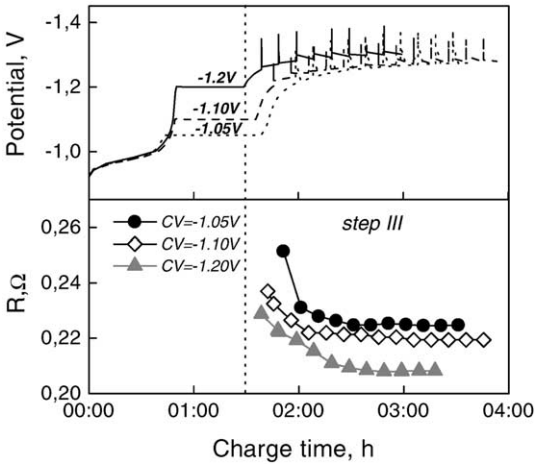

Fig. 10. Internal resistance changes during the third constant current step in the I_1, φ_2, I_3 mode.

3.7. Structure of NAM after the second and the third charge steps

Scanning electron micrographs of the negative active mass after the end of the second and the third steps of charge are presented in Fig. 11. At the end of the second step, some unreduced $PbSO_4$ crystals can be observed, which are no longer detected in the micrograph after the end of the third step. Obviously, the final constant current step ensures complete recharge of the negative active material.

The reduction of $PbSO_4$ proceeds in the presence of an expander, which is a surface active polymer. The expander can suppress the dissolution of lead sulfate during charge and on the other hand can affect the kinetics deposition of Pb atoms by preferential blocking of the active centers on the electrode surface. During the third charge step, the evolved hydrogen probably invokes desorption of the expander, and thus favors the dissolution of the remaining $PbSO_4$ crystals on the electrode surface.

3.8. Influence of the φ_2 potential on the capacity and cycle life of the negative plate

The influence of the potential, φ_2 during the second charge step on the cycle life and the capacity of the negative electrode was studied. Fig. 12 shows the potential transients obtained when the model electrode was charged employing the three-step algorithm. The potential during the second step varied. The initial charge current was 1 C and the final was 0.05 C.

The influence of the charge potential φ_2 during the second step, on the cycle life of the negative electrode is illustrated in Fig. 13. The cycle life of the model electrode depends on the potential during the second charge step. When at the second charge step, the negative electrode is polarized to potentials more negative than -1.10 V the cycle life decreases. A possible explanation of this effect could be the hydrogen evolution at higher potentials during the

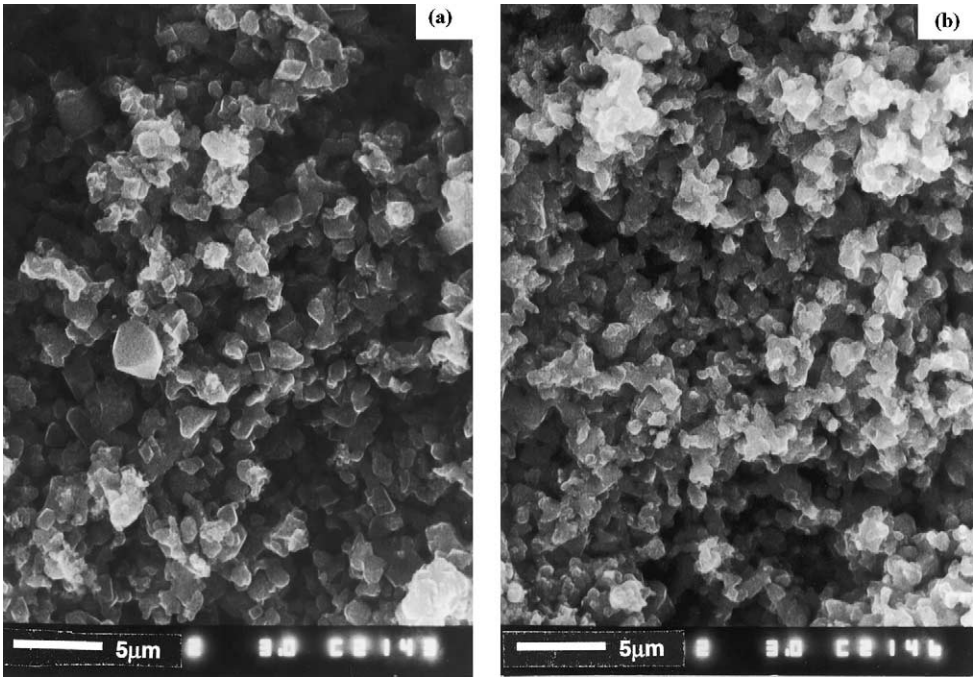

Fig. 11. SEM micrographs of the negative electrode, I_1, φ_2, I_3 charge mode: (a) end of second step; (b) end of third step.

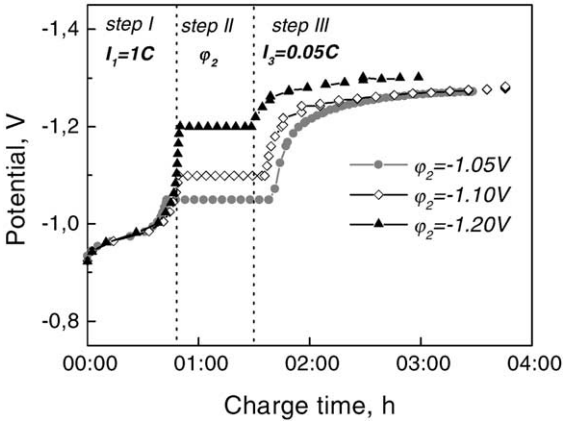

Fig. 12. Potential/time transients on I_1, φ_2, I_3 charge with different potentials φ_2.

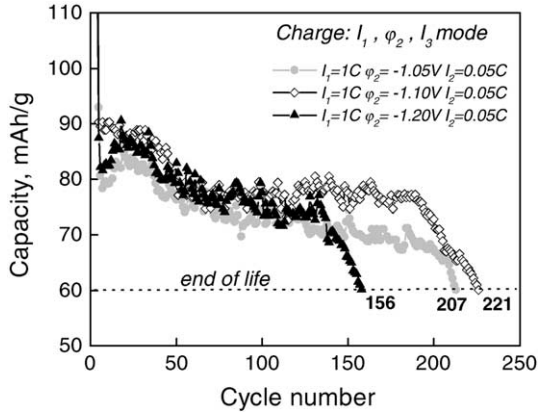

Fig. 13. Influence of the charge potential φ_2 on the cycle life of the negative electrode.

second step, which causes expansion of the negative active material and loss of connection between the lead crystals. Secondly, according to the mechanism presented above, the process of reduction of $PbSO_4$ remaining after the first step to Pb requires lower overpotentials.

4. Conclusions

The charge algorithm employed for charging lead–acid cells exerts a strong effect on the capacity and cycle life of the negative electrodes. The following conclusions can be drawn on the basis of the results obtained:

- With increase of the current during the first step of charge, the capacity of the negative electrode decreases and the cycle life shortens. This phenomenon is reversible, as it is due to incomplete reduction of $PbSO_4$ to Pb, i.e. to residual sulphation of the plate. A mechanism for the incomplete reduction of $PbSO_4$ to Pb is proposed. The reason for this effect of the high charge current is slower diffusion of the H_2SO_4 from the pores of the negative plate towards the bulk solution. This causes the concentration of sulfuric acid inside the NAM pores to increase and hence the solubility of $PbSO_4$ decreases. The concentration of Pb^{2+} ions involved in the electrochemical reaction decreases and the charge acceptance of the negative plate declines.
- The higher initial charge current influences markedly the formation of smaller Pb crystals that build up the energetic structure of the negative active material.
- It is essential to include a third step with a small constant current in the charge algorithm, so as to ensure complete

charge of the electrode and to reduce the resistance of the negative plate.

References

[1] P.T. Moseley, J. Power Sources 95 (2001) 218.
[2] T.G. Chang, D.M. Jochim, J. Power Sources 91 (2000) 177.
[3] M. Fernandez, F. Trinidad, J. Power Sources 67 (1997) 125.
[4] F. Trinidad, F. Saez, J. Valenciano, J. Power Sources 95 (2001) 24.
[5] D. Berndt, J. Power Sources 100 (2001) 29–46.
[6] R.F. Nelson, J. Power Sources 73 (1998) 104.
[7] R.F. Nelson, E.D. Sexton, J.B. Olson, M. Keyser, A. Pesaran, J. Power Sources 88 (2000) 44.
[8] D. Pavlov, G. Petkova, M. Dimitrov, M. Shiomi, M. Tsubota, J. Power Sources 87 (2000) 39.
[9] G.W. Vinal, D.N. Graig, J. Res. Nat. Bur. Stand. 22 (1939) 55.
[10] V. Danel, V. Plichon, Electrochim. Acta 27 (1982) 771.
[11] D. Pavlov, G. Papazov, B. Monahov, J. Power Sources 113 (2003) 255–270.
[12] D. Pavlov, V. Iliev, J. Power Sources 7 (1981) 153.